SIMPLIFIED NUMERICAL MODELS FOR MICROWAVE DOSIMETRY IN HUMAN TISSUE

M. Morega*, Al. M. Morega* and A. Machedon

POLITEHNICA Univ. of Bucharest, Department of Electrical Engineering, Bucharest, Romania
* IEEE Member

mihaela@iem.pub.ro

Abstract: Exposure of living bodies to very high frequency non-ionizing electromagnetic field (EMF) (i.e. microwave (MW) domain, (10^8 – 10^{11}) Hz) is associated to the use of mobile communications, radar detection, dielectric heaters and to several medical procedures. Artificial materials with electric properties similar to those of anatomical tissues are used in experimental procedures for electronic equipment certification. Numerical modeling is also a powerful tool for EMF distribution and dosimetric parameters evaluation, while an optimum between computational costs and relevance of results is desirable. The main objective of this work is to propose some quantitative criteria concerning the correspondence between numerical models used in computation and physical models (phantoms) used in measurements for MW macroscopic dosimetry assessment. Several 2D and 3D finite element (FEM) models are developed and EMF parameters are computed for different inner structures and heterogeneity levels of the exposed body. The general characteristics of the MW source and the exposed medium are associated to mobile telephony conditions, but the methods could be also extended to other applications. The equivalent electric properties for simplified models are evaluated through equivalence concerning the EMF distribution, between the heterogeneous anatomical structure and the corresponding homogeneous one.

Introduction

Localized human exposure to low power near field in the MW frequency range is associated to the use of wireless technology and to medical procedures based on hyperthermia.

Microwave dosimetry consists of three categories of problems [1]:

(1) specification of the exposure conditions: EMF source and characteristics of the target body (shape and inner structure – heterogeneity and physical properties),

(2) determination of the so-called internal fields, namely the electric and magnetic fields distributions inside the body exposed to the incident fields,

(3) estimation of the biological effects.

An antenna, usually placed near the surface of the skin, is the EMF source. Excited with electromagnetic radiation in the MW domain, biological tissues are materials that behave, at a macroscopic scale, as lossy dielectrics; the depth of penetration is limited in those circumstances to 0.02 – 0.03 m. Consequently, the exposure of living bodies to very high frequency non-ionising EMF may lead to significant absorption of energy mainly localized at the surface of the exposed body. The energy absorption is related to thermal effects and is usually quantified by the Specific energy Absorption Rate ($SAR = \sigma E_{\max}^2 / (2\rho)$ where $E_{\max}$ is the maximum value of the time harmonic strength of the electric field **E**, σ is the electric conductivity and ρ is the mass density of the exposed tissue). Thermal biological effects are intensively studied and documented; currently, limiting exposure restrictions are exclusively based on thermal effects. However, athermal physiologic phenomena are suspected to occur and make the object of important but yet inconclusive research in this field.

Experimental evaluation and computation of EMF distribution inside the exposed body are the two ways that allow the investigation of dosimetric parameters. Macroscopic analysis generates data on the distribution of the EMF inside the exposed body and opens the path for microscopic dosimetry. Inner electric field is measured either in experimental animals or in models (phantoms) which consist of materials that have electric and magnetic properties similar to that of animal tissue; the measurements follow standard protocols in order to minimize the uncertainties. The numerical modeling allows detailed description of the exposure conditions and sophisticated processing of data, but is highly dependent on expensive computational resources. The usefulness of numerical modeling as well as measurements inside the body is beyond doubt for the assessment of biological effects necessary for setting the safety exposure guidelines; the two evaluation tools could complement each other in the design of harmless MW devices and in the development of certification protocols.

The objective of our research is to present and validate simplified numerical models for dosimetric studies in the MW domain of the EMF. This work is focused on the construction of a 3D model adequate for the study of EMF penetration and dosimetric estimates in the head of a cellular phone user, but the followed path and the tools are adequate for any other application. The 3D human head model presented here

ISSN: 1727-1983

has a realistic shape, obtained through geometrical reconstruction from 2D tomographic slices. Its inner structure is represented by a homogeneous tissue with equivalent physical properties. We show in this paper the construction of the 3D geometry, the computation of the equivalent dielectric properties and some dosimetric estimates.

Materials and Methods

The 3D reconstruction of the human head [2] is accomplished with the aid of the Matlab – Femlab software suite [3], after the preprocessing of the data with 3D Slicer [4]. Femlab is an interactive environment for modeling and solving FEM based problems, while 3D Slicer is an image processor, capable of volumes reconstruction from 2D slices. The primary data used are CT images scanned from an adult person, as a series of cross-sectional images made along an axis, a few millimeters one of another; a set of such images is called a *volume*. The images are segmented (the regions of interest are identified on the image – in our case the whole head) using a combination of manual and semiautomatic segmentation (the Threshold and Draw modules of 3D Slicer). From these images the head is reconstructed in 3D Slicer as fig. 1 shows.

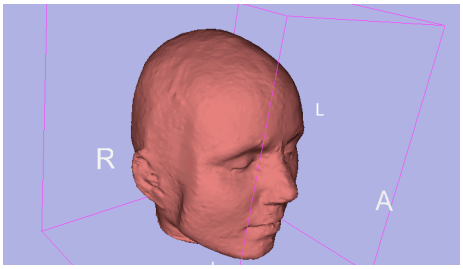

Figure 1: The head, reconstructed in 3D Slicer

The images segmented in 3D Slicer were used as the basis of the reconstruction in Matlab. Each image from the segmented volume is saved in a separate file, the information in each one being coded as a string of two octets (raw image format). Those images are imported in Matlab using a custom script (to automate the process). Using several Matlab and Femlab functions [3] (flim2curve, solid2, geomdel, geomcomp, loft and other custom scripts), the final object is rendered in Femlab. A conventional half wavelength center fed dipole antenna is located near the right ear; the outer domain, the space around the head, is limited with a sphere (fig. 2).

Computational resources impose restrictions for the representation of the head anatomical structure. An inner structure described by thinn tissue layeres, like the one presented in [5], requires large computer memory for the discretization mesh, which proves to be an excessive demand for our available resources.

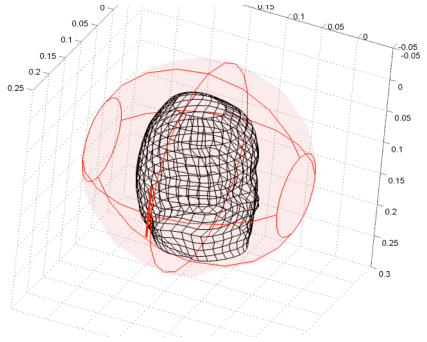

Figure 2: Human head geometry in FEMLAB

The solution to this problem is a compromise. We computed equivalent dielectric properties by energetic equivalence between the EMF distributions in a six tissues layered structure and in a homogeneous one. The equivalence is performed on 2D models reduced from 3D based on axial symmetry hypothesys. Fig. 3 sugests the assumptions made here: (a) the geometrical configuration could be approximated with elipsoidal and spherical layers; (b) the axial symmetry, adequate for the antenna, proves to be also suitable for a practical, even unrealistic, anatomical structure.

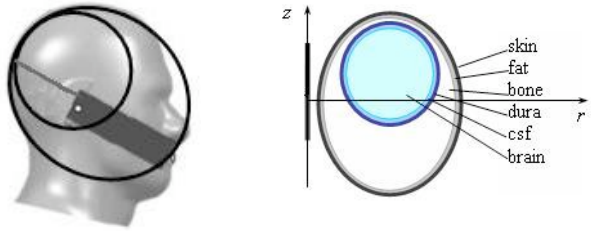

a. Typical configuration b. 2D model (6 layers)

Figure 3: Computational 2D domain based on a multi-layered structure

The numerical computation used for the 2D FEM model is based on the Femlab software [3], the *Electromagnetics Module*, in the *axisymmetric transversal magnetic (TM) waves* application mode, *time-harmonic* submode. The wave equations are applied for lossy media, characterized by the complex electric permittivity $\underline{\varepsilon}$

$$\nabla\times\left(\frac{1}{\mu_0}\nabla\times\underline{\mathbf{E}}\right)-\omega^2\underline{\varepsilon}\underline{\mathbf{E}}=0\,,$$

$$\nabla\times\left(\frac{1}{\underline{\varepsilon}}\nabla\times\underline{\mathbf{H}}\right)-\omega^2\mu_0\underline{\mathbf{H}}=0\,, \tag{1}$$

where the unknown field variables, in the cylindrical coordinate system and in complex form are:

$$\underline{\mathbf{H}}(r,z,t)=\underline{H}_\varphi(r,z)\mathbf{e}_\varphi e^{j\omega t}\,,$$

$$\underline{\mathbf{E}}(r,z,t)=\left(\underline{E}_r(r,z)\mathbf{e}_r+\underline{E}_z(r,z)\mathbf{e}_z\right)e^{j\omega t}\,. \tag{2}$$

ISSN: 1727-1983

The computational domain is limited with *low-reflecting* boundary conditions

$$\mathbf{n}\times\left(\frac{\varepsilon}{\mu_0}\right)^{1/2}\underline{\mathbf{E}}-H_\varphi=-2H_{\varphi 0},\ H_{\varphi 0}=0 \qquad (3)$$

and the boundary on the (Oz) axis satisfies *axial symmetry* conditions

$$E_r=0,\quad \frac{\partial E_z}{\partial r}=0,\quad \frac{\partial H_\varphi}{\partial r}=0. \qquad (4)$$

The EMF source is introduced through a nonhomogeneous *magnetic field* boundary condition, simulating the center fed dipole antenna.

The Femlab linear stationary solver is based on Gaussian elimination. The FEM mesh is composed of triangular elements, and for its density assessment were performed two accuracy tests: the constant radiated power and an energetic balance (the radiated power compared with the sum of the power absorbed in the head and the power radiated in the antenna far field).

Fig. 4 presents the dielectric properties, electric conductivity and dielectric permittivity, taken from literature [6], for the frequency range used in cellular phone technology.

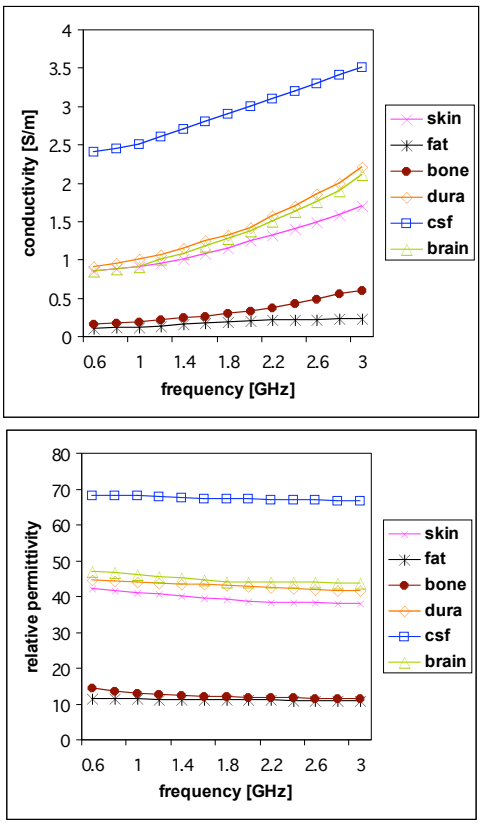

Figure 4: Frequency dependence of the electric conductivity (up) and dielectric permittivity (down) for the model of a human head with six tissue layeres

The dielectric properties of the reduced homogeneous model (σ_{equiv} respectively ε_{equiv}) are computed by energy based equivalence, considering that the total absorbed power and total electric energy have the same values in the heterogeneous (composed by i different sub-domains) and equivalent homogeneous models:

$$\int_i \sigma_i (E_i)^2\,\mathrm{dv}=\sigma_{equiv}\int_i (E_i)^2\,\mathrm{dv}, \qquad (5)$$

$$\int_i \frac{1}{2}\varepsilon_i (E_i)^2\,\mathrm{dv}=\frac{1}{2}\varepsilon_{equiv}\int_i (E_i)^2\,\mathrm{dv}. \qquad (6)$$

The equivalent mass densities, necessary for dosimetric estimates, are approximated by weighted arithmetic mean.

The method presented above is applied to compute the equivalent dielectric properties of two reduced head models [7] suggested in fig. 5:
- reduced, heterogeneous model, two sub-domains: *equivalent skull* (skin+fat+bone) and *equivalent brain* (dura+csf+brain);
- reduced, homogeneous model: *equivalent head* tissue.

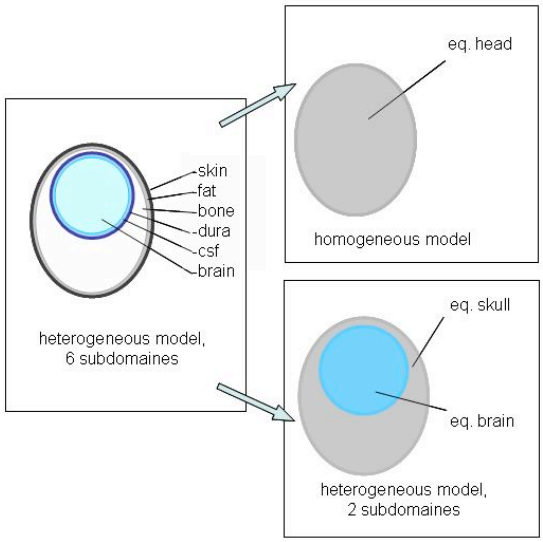

Figure 5: Reduced head models

Fig. 6 shows the frequency dependence of the equivalent dielectric properties: conductivity (up) and permittivity (down), in the considered frequency range.

The 3D FEM models used in this wok are based on the same equations (1); the Femlab *3D Electro-magnetic Waves* application mode [3] is used; the boundary conditions and the solver options are similar to those specified for the 2D FEM models.

Results and Discussion

For the soundness of the referred 2D FEM models based on axial symmetry, we first present a comparison between a 3D analytical model introduced in [5] (with a spherical layered structure described by fig. 7 and table 1), and a 2D FEM model similar in structure, described by the equations (2) – (4).

ISSN: 1727-1983

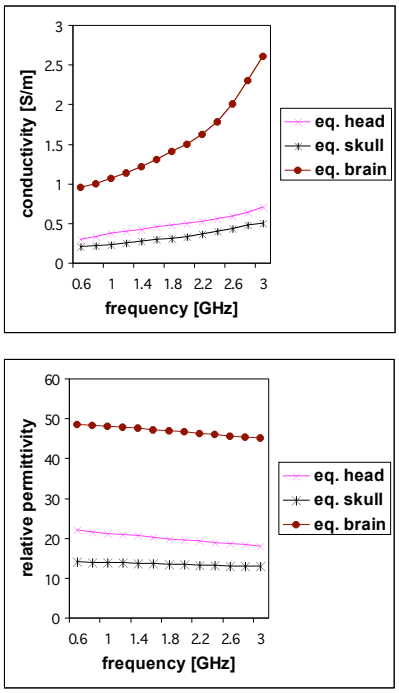

Figure 6: Frequency dependence of the equivalent dielectric properties

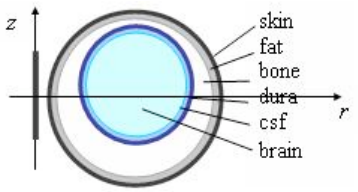

Figure 7: Computational domain structure similar to [5] (layered eccentric 6-spheres model)

Table 1: Characteristics of tissue sub-domains [5]

Tissue	Radius [mm]	Density [kg/m^3]	Conductivity [S/m]		Relative permittivity	
			0.9 GHz	1.8 GHz	0.9 GHz	1.8 GHz
skin	90	1100	0.87	1.18	41.4	38.9
fat	89.3	920	0.11	0.19	11.3	11
bone	87.7	1850	0.14	0.28	12.5	11.8
dura	67.2	1050	0.96	1.32	44.4	42.9
c.s.f.	66.7	1060	2.41	2.92	68.7	67.2
brain	64.7	1030	0.86	1.27	46.5	43.9

Two categories of global parameters (absorbed power and averaged *SAR* in each tissue) were computed with the 2D FEM model, and the results were compared with similar estimates presented in [5], based on analytical calculus. Table 2 shows the power absorbed in each tissue, as a percentage of the total absorbed power and table 3 shows the averaged *SAR* in each tissue divided by the total absorbed power. Two MW frequencies (0.9 and 1.8 GHz) were considered. The reference data are taken from graphs (figs. 4a and 5a) presented in paper [5].

Table 2: Power absorbed in each tissue as a percentage of the total absorbed power 100 P / P_{total} [%]

P/P_{total} [%]	0.9 GHz		1.8 GHz	
	model in paper [5]	**2D FEM model**	model in paper [5]	**2D FEM model**
skin	9	**9.4**	9	**8.7**
fat	3	**2.8**	3	**2.7**
bone	30	**31.4**	48	**50.2**
dura	2	**1.3**	2	**1.2**
c.s.f.	12	**11.9**	10	**9.5**
brain	43	**43.2**	28	**27.7**

Table 3: Averaged SAR in each tissue divided by the total absorbed power SAR / P_{total} [W/kg per W]

SAR/P_{total} [W/kg per W]	0.9 GHz		1.8 GHz	
	model in paper [5]	**2D FEM model**	model in paper [5]	**2D FEM model**
skin	0.168	**0.163**	0.112	**0.112**
fat	0.026	**0.025**	0.023	**0.024**
bone	0.015	**0.013**	0.016	**0.021**
dura	0.059	**0.044**	0.037	**0.037**
c.s.f.	0.143	**0.103**	0.081	**0.078**
brain	0.049	**0.024**	0.023	**0.015**

A fairly good agreement could be observed for the compared data. The 2D FEM model, based on axial symmetry, is not derived from a realistic anatomy. However, it represents a very useful and economic tool in modeling cross-sections of a 3D body, particularly in computing global parameters. The main quantitative difference in the EMF distribution between the 3D and the axial-symmetric 2D models comes from the *coupling factor*, defined as the ratio between the power absorbed in the head and the power emitted by the source. In the 2D case, this *coupling factor* decreases slightly from the unit value with the growth of the distance between the antenna and the body (in the range of small distances, comparable to the wavelength), while in the 3D case it is strongly dependent on that distance. Fig. 8 displays the *coupling factor* dependence on the distance between the antenna and the head, computed at 1.8 GHz, for a 3D homogeneous model, with ellipsoidal shape and the corresponding 2D model.

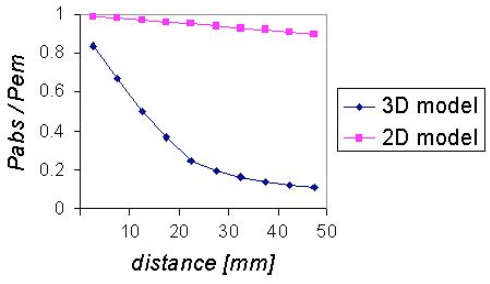

Figure 8: *Coupling factor* versus antenna-head distance

ISSN: 1727-1983

An evaluation of the results produced by axial-symmetric 2D and by 3D models is presented in fig. 9, where the electric field strength (E) distribution along the maximal values direction (r) is presented for: a 6-layers 2D structure, an equivalent 2-layers 2D structure, a homogeneous equivalent 2D structure and a homogeneous equivalent 3D structure. The equivalent properties are taken from fig. 6; the antenna is placed at 10 mm near the head and the emitted power is 1W, at the frequency 1.8 GHz.

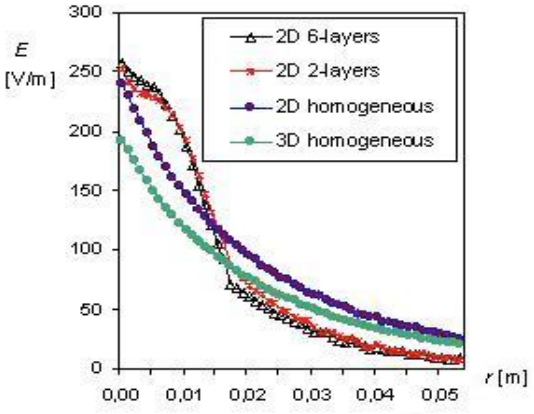

Figure 9: E distribution (maximal time-harmonic values) versus distance r, measured from the surface of the skin, for 2D and 3D FEM models

The good agreement among the 2D models is evident and the E-values for the 3D model are lower by approx. the square root of the *coupling factor* than for the corresponding 2D (homogeneous) model. In order to use the 2D model for the evaluation of local data (E or SAR) distribution, one should consider the *coupling factor* for scaling the results.

For dosimetric evaluations we propose here and compare three 3D FEM models, based on the geometries and structures referred earlier:

- model A - homogeneous model with the head reconstructed from tomographic slices (shown in fig. 2), filled with *equivalent head* material (fig. 6),
- model B – homogeneous model with ellipsoidal head, filled with *equivalent head* material (fig. 6),
- model C – heterogeneous model with ellipsoidal *equivalent skull* and spherical *equivalent brain* (fig. 6).

E and SAR calculated for model A are displayed in the longitudinal and transversal section planes. Fig. 10 shows the E-field colored maps (maximal values in the time-harmonic mode) and fig. 11 displayes the SAR spectra inside the head. The dipole antenna is located at 5mm from the head and delivers 0.125 W at 1.8 GHz.

The guidelines formulated by the International Commission on Non-Ionizing Radiation Protection limit the localized (head and trunk) human exposure to EMF with the basic restriction for this type of exposure, the averaged value of SAR for 10g of tissue ($SAR_{\max\ 10g}$); this value should not exceed 2 W/kg (for the general public). In our example $SAR_{\max\ 10g}$ = 1.5 W/kg.

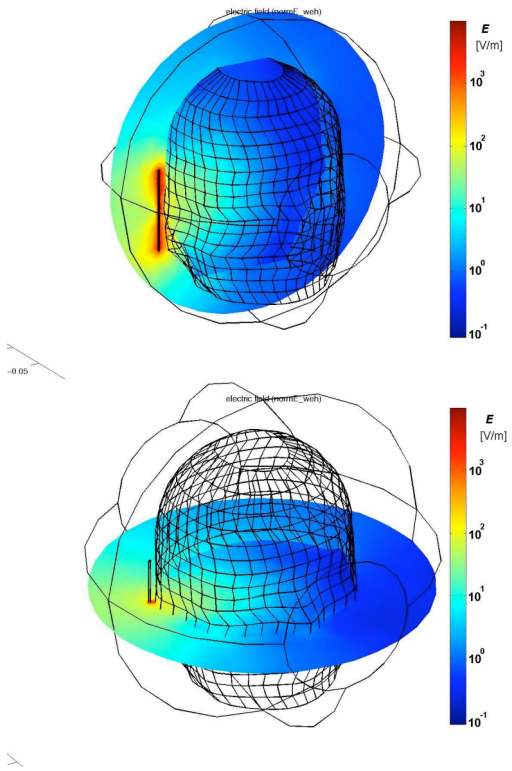

Figure 10: The electric field strength E in section planes longitudinal (up) and transversal (down) with reference to the antenna

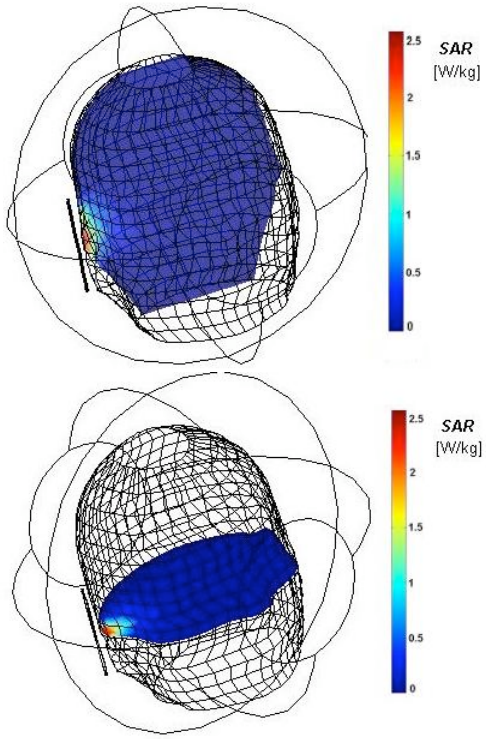

Figure 11: SAR distribution in the head in section planes longitudinal (up) and transversal (down) with reference to the antenna

ISSN: 1727-1983

A comparison of the results obtained with the three types of 3D FEM models mentioned earlier (A, B, C) is evidenced by fig. 12, which shows the distribution of the electric field strength *E* (maximal time-harmonic values) inside the head model, along an axis with maximal values (this axis marks the intersection between the two section planes taken into consideration in figs. 10 and 11. The distance between the antenna and the head is 5mm and the power emitted by the antenna is 0.125 W at 1.8 GHz.

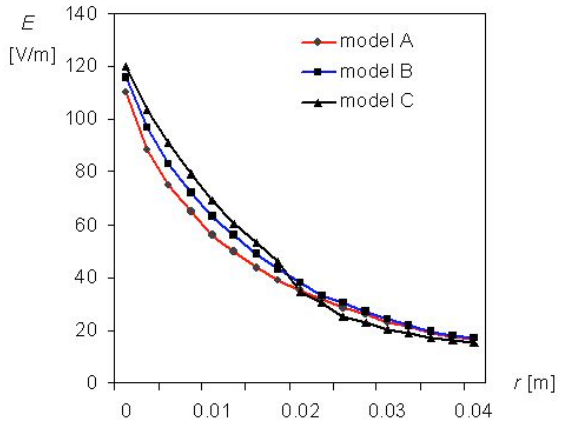

Figure 12: *E* distribution (maximal time harmonic values) versus distance *r*, measured from the surface of the skin, for 3D FEM models

Models A and B differ with regard to the shape of the head and have the same inner equivalent material properties. *E* - field values for model A (the realistic head) are lower than for model B (the ellipsoidal head) because it presents a larger curvature at the incidence of the electric field. *E* - field distribution for model C is sensitive to the heterogeneity of the domain. The three models give similar outputs and any of them could be used in simplified computation and for validation of experimental measurements on head phantoms.

Conclusions

The construction of the simplified 2D FEM models arise from the necessity to evaluate EMF parameters distribution in layered structures like anatomical tissues when exposed to MW either in day-to-day activities (as mobile phone use) or in medical therapy (hyperthermia, stimulation, etc.). Compared with more sophisticated models, the 2D FEM models demonstrate advantages in economy of resources, accessibility and rapidity, while the results are sufficiently accurate for global estimates and for comparison with experimental *SAR* and *E* distributions from measurements on phantom human models. The results presented here are specific for the conditions related to mobile phone use near the head, but the method of equivalence between the heterogeneous anatomical structures and the homogeneous equivalent domains could be also applied to other parts of the body. The results are useful for the optimal design of 3D models.

We have proposed a quantitative correspondence between numerical models and physical models (phantoms) used in measurements for microwave macroscopic dosimetry assessment. In the evaluation of EMF penetration in tissue exposed to microwaves the *E* and *SAR* distributions were determined. Our results show that the inner distribution of the electric field has a low sensitivity to the dispersion of dielectric properties (in reasonable limits usual for practical situations) and to the heterogeneity level of the anatomical structure. In numerical and experimental modeling of the human body exposure to ELF in the MW range it is important to reproduce the external shape of the body, but the models could be simplified in their inner structure.

The advantages of the numerical modelling compared with experimental measurements are obvious: rapidity in evaluation and versatility of the models - in numerical models the anatomical data could be easily changed. Besides, in experimental studies the required laboratory conditions (anechoic chamber, adequate phantom model and sophisticated instruments) are seldomly accesible.

References

[1] DURNEY, C. H., CHRISTENSEN, D. A. (2000): 'Basic Introduction to Bioelectromagnetics', (CRC Press LLC)

[2] SAMFIRESCU, S., MOREGA, M. (2004): '3D Reconstruction of the Human Head', Proc. of ATEE 2004 – 4th Intl. Symp. on Advanced Topics in Electrical Engineering, Bucharest, Romania, CD-ROM, ISBN 973-7728-31-9

[3] COMSOL AB., FEMLAB 2.3 (2002), 3 (2004): 'Users Guide. Electromagnetics Module', Stockholm, Sweden

[4] 3D Slicer 1.3.0. (2002): 'Medical Visualization and Processing Environment for Research', Open source development project, http://www.slicer.org

[5] MONEDA, A. P., IOANNIDOU, M. P., CHRISSOULIDIS, D. P. (2003): 'Radio-Wave Exposure of the Human Head: Analytical Study Based on a Versatile Eccentric Spheres Model Including a Brain Core and a Pair of Eyeballs', *IEEE Trans. Biomed. Eng.*, **50**, pp. 667- 676

[6] GABRIEL, C., GABRIEL, S. (2002): 'Dielectric Properties of Body Tissues at RF and Microwave Frequencies', Report for Armstrong Laboratory (AFMC), Occupational and Environmental Health Directorate - RF Radiation Division, USA

[7] MOREGA, M., MACHEDON, A., SAMFIRESCU, S. (2004): 'Dielectric Properties in Numerical Models of Biological Tissues for Applications in Microwave Dosimetry', Proc. of MMDE 2004 - 4th Intl. Workshop on Materials for Electrotechnics, Bucharest, Romania, ISBN 973-718-006-2, paper D – O2 – D04, p. 250-255.

ISSN: 1727-1983